
Domain-Irrelevant Representation Learning for Unsupervised Domain Generalization

Xingxuan Zhang, Linjun Zhou, Renzhe Xu, Peng Cui*, Zheyang Shen, Haoxin Liu

Department of Computer Science, Tsinghua University, Beijing, China

xingxuanzhang@hotmail.com, zhoulj16@mails.tsinghua.edu.cn,

xrz199721@gmail.com, cui@tsinghua.edu.cn,

shenzy17@mails.tsinghua.edu.cn, 1132462715@qq.com

Abstract

Domain generalization (DG) aims to help models trained on a set of source domains generalize better on unseen target domains. The performances of current DG methods largely rely on sufficient labeled data, which however are usually costly or unavailable. While unlabeled data are far more accessible, we seek to explore how unsupervised learning can help deep models generalize across domains. Specifically, we study a novel generalization problem called unsupervised domain generalization, which aims to learn generalizable models with unlabeled data. Furthermore, we propose a Domain-Irrelevant Unsupervised Learning (DIUL) method to cope with the significant and misleading heterogeneity within unlabeled data and severe distribution shifts between source and target data. Surprisingly we observe that DIUL can not only counterbalance the scarcity of labeled data, but also further strengthen the generalization ability of models when the labeled data are sufficient. As a pretraining approach, DIUL shows superior to ImageNet pretraining protocol even when the available data are unlabeled and of a greatly smaller amount compared to ImageNet. Extensive experiments clearly demonstrate the effectiveness of our method compared with state-of-the-art unsupervised learning counterparts.

1 Introduction

Deep neural networks based approaches have achieved striking performance in tasks where training data and test data share similar distribution. However, under considerable distribution shifts, they can significantly fail [3, 14, 25, 47, 53]. To address this problem, the literature in domain generalization (DG) proposes algorithms that have access to labeled data from multiple domains or environments during training and generalize well to unseen test domains [16, 30, 32, 34, 41, 60].

Sufficient labeled data are crucial for current DG methods. A common and effective approach to address DG problems is to enlarge the available data space with augmentations of source domains [4, 64, 65]. With sufficient source data and strong augmentations, even ERM can outperform previous state-of-the-art methods [19]. Nevertheless, both augmentation-based methods and carefully hyperparameter tuned ERM assume an adequate amount and strong heterogeneity of available data for representation learning. As manually labeled data can be costly or unavailable while unlabeled data are far more accessible, we study a novel generalization problem called unsupervised domain generalization (UDG) to learn visual representations that generalizes well across domains in unsupervised manner to reduce the dependence of DG methods on labeled data.

Recently, the research community has spent significant effort to develop algorithms for learning visual representations without category labels [20, 48, 61] and shows the advance of contrastive

*Corresponding author, also with Beijing Key Lab of Networked Multimedia.
Preprint. Under review.

learning based approaches compared to other unsupervised counterparts [22, 54]. In contrastive learning literature [2, 24, 26, 43, 62], a pair of samples is a positive pair only if they originate from the same image and the others are negative pairs [5, 7]. The objective of contrastive learning is to make each sample similar to its positive matching and dissimilar to others. Thus perturbation robust representations are learned under I.I.D hypothesis. However, the heterogeneity caused by domain shifts in training data is significant and can not be fully counterweighed via data transformations in the DG problem (for instance, one can hardly transform a dog in sketch to photo), inducing models to leverage the domain related features to distinguish one sample from its negatives [1, 50]. While the objective of DG is to learn an invariant representation space where dissimilarity across domains is minimized [39, 41]. The inconsistency between contrastive learning and the objective of DG causes two drawbacks: 1) A large proportion of negative pairs showing the dissimilarity across domains reduce training efficiency; 2) When the correlations between domains and categories are strong and misleading, the model may tend to utilize domains related features instead of predictive features in the inference phase [63]. Thus current contrastive learning can not perfectly handle the UDG problem.

To address this problem, we propose Domain-Irrelevant Unsupervised Learning (DIUL), a novel unsupervised learning algorithm for domain generalization which unifies both objectives of DG and contrastive learning. To force the model ignore domain related features, we select valid sources of negative samples for any given queue according to the similarity between different domains. Specifically, the more similar two domains are, the more likely two samples in a negative pair are selected from these two domains, respectively. In extreme cases, the algorithm degenerates into only selecting negative samples within the same domain with a given sample. Intuitively, when a negative pair comes from a single domain, domain related features can not be used to distinguish two samples, thus domain irrelevant representations are learned with contrastive loss.

Unsupervised pretraining protocol achieves a significant improvement in generalization, indicating that the UDG problem is meaningful and enlightening for DG. We further show that DIUL outperforms state-of-the-art counterparts by a considerable margin with quantitative and qualitative experiments. Moreover, prepositive unsupervised learning can be considered as a protocol of pretraining. Although initialization of weights pretrained on ImageNet shows unparalleled effectiveness on independent and identically distributed (I.I.D.) tasks, we argue that it lacks rationality for the DG problem. Since ImageNet can be considered as a set of data sampled from latent domains, the distribution shifts across domains are not as significant as most DG datasets [23], resulting in insufficient heterogeneity for models to learn a generalizable representation space. Thus the protocol of unsupervised pretraining on heterogeneous unlabeled data is a reasonable alternative to initialization with weights pretrained on ImageNet for DG.

2 Related work

Domain Generalization. Domain generalization (DG) considers the generalization ability to novel domains of deep models trained on source domains where the heterogeneity caused by domain shifts is significant. A common approach is extracting domain-invariant features over multiple source domains [11, 16, 28, 30, 33, 35, 40, 45, 49, 63] or aggregating domain-specific modules [37, 38] to conduct domain-invariant or domain specific. Many works propose to enlarge the available data space with augmentation of source domains [4, 12, 46, 51, 64, 65]. There are several approaches that exploit regularization with meta-learning [11, 34] and Invariant Risk Minimization (IRM) framework [1] for DG. Despite the promising results achieved by current DG methods, all of them assume that the training data provide ample heterogeneity and knowledge for target categories. Such assumptions hinder DG methods from real applications.

Unsupervised learning. Unsupervised representation learning generally involve two categories, namely generative and discriminative [7, 8]. Many of generative approaches rely on auto-encoder [59] or adversarial learning [17], where data and representations are jointly modeled [9, 13, 15]. There are some self learning methods relying on auxiliary handcrafted prediction tasks such as image jigsaw puzzle[42] and geometric transformations[10] to learn representations. Among discriminative method, Contrastive loss based approaches forces representation of different views of the same image closer with spreads representations of views from different images apart and achieves current state-of-the-art performance [5, 18, 22, 24, 27, 43, 55] . As designed for problems under the I.I.D assumption, current contrastive learning can not distinguish domain or category related features,

resulting in low training efficiency or misleading by spurious correlations between categories and domains.

3 Methods

3.1 Problem Formulation

Notations Let \mathcal{X} be the feature space, \mathcal{Y} the category label space, and \mathcal{D} the domain label space. Accordingly, we use X, Y, D to denote the random variables which take values in \mathcal{X}, \mathcal{Y} and \mathcal{D} . A dataset S contains N_S samples $\{X_i, y_i, d_i\}_{i=1}^{N_S}$ sampled from a joint distribution P^S on $\mathcal{X} \times \mathcal{Y} \times \mathcal{D}$. Let P_X^S, P_Y^S and P_D^S denote the marginal distribution of P^S on X, Y, D respectively. Let $\text{Supp}(\cdot)$ denote the support of a distribution. For example, $\text{Supp}(P_X^S)$ denotes the support of distribution P_X^S . We describe datasets as labeled when the category labels are available while others as unlabeled. We aim to learn a model generalizable to any unknown testing dataset. Formally, the problem is defined as follows:

Problem 3.1 (Unsupervised Domain Generalization). Let $S_{UL} = \{X_i, d_i\}_{i=1}^{N_L}$ be the unlabeled dataset with N_{UL} samples from distribution $P^{S_{UL}}$ and $S_L = \{X_i, y_i\}_{i=1}^{N_L}$ be the labeled dataset with N_L samples from distribution P^{S_L} . There exists an unknown testing distribution $P^{S_{test}}$ that satisfies

$$\text{Supp}\left(P_D^{S_{test}}\right) \cap \left(\text{Supp}\left(P_D^{S_{UL}}\right) \cup \text{Supp}\left(P_D^{S_L}\right)\right) = \emptyset. \quad (1)$$

$$\text{Supp}\left(P_Y^{S_{test}}\right) = \text{Supp}\left(P_Y^{S_L}\right). \quad (2)$$

Given S_{UL}, S_L and a loss function $\ell(X, Y; \theta)$, we aim to learn a model with parameters θ that achieves best performance on $P^{S_{test}}$.

$$\theta^* = \arg \min_{\theta} \mathbb{E}_{(X, Y, D) \sim P^{S_{test}}} [\ell(X, Y; \theta)]. \quad (3)$$

Remark 3.1 (Explanation of the two constraints). Following standard DG setting, Equation 1 requires that there is no domain overlap between testing and all available training data including the unlabeled dataset and labeled dataset. Meanwhile, Equation 2 requires that the category space should be the same between testing dataset and the labeled dataset.

This setting is sound, since we can consider the source or mechanism of data generation as the domain while the latent structure of data other than domains determines the categories. Accordingly, the domain label is significantly easier to access while category labeling can be expensive, leading a large scale of data with domain label while without category label.

UDG settings We specifically describe all possible 4 settings that support unsupervised domain generalization (UDG) according to the intersections in the category and domain spaces between unlabeled and labeled data, namely *all correlated, domain correlated, category correlated, uncorrelated*.

All correlated. $\text{Supp}(P_D^{S_{UL}}) = \text{Supp}(P_D^{S_L}), \text{Supp}(P_Y^{S_{UL}}) = \text{Supp}(P_Y^{S_L})$.

When the data are partially and randomly labeled, the unlabeled and labeled data are homologous so that there can be overlap in the category and domain spaces between them.

Domain correlated. $\text{Supp}(P_D^{S_{UL}}) = \text{Supp}(P_D^{S_L}), \text{Supp}(P_Y^{S_{UL}}) \cap \text{Supp}(P_Y^{S_L}) = \emptyset$.

A more challenging but common setting is that unlabeled and labeled data share the same domain space while there is no overlap between the category space of unlabeled and labeled data.

Category correlated. $\text{Supp}(P_D^{S_{UL}}) \cap \text{Supp}(P_D^{S_L}) = \emptyset, \text{Supp}(P_Y^{S_{UL}}) = \text{Supp}(P_Y^{S_L})$.

Similar with *domain correlated*, this setting assumes that unlabeled and labeled data share the same category space while there is no overlap between the domain space of unlabeled and labeled data.

Uncorrelated. $\text{Supp}(P_D^{S_{UL}}) \cap \text{Supp}(P_D^{S_L}) = \emptyset, \text{Supp}(P_Y^{S_{UL}}) \cap \text{Supp}(P_Y^{S_L}) = \emptyset$.

When extra data from the same sources (domains) as labeled data are unavailable, there may be no overlap between the category and domain spaces of unlabeled data and labeled data, resulting in the most challenging and flexible setting.

3.2 Domain-irrelevant unsupervised learning

We propose the domain-irrelevant unsupervised learning (DIUL) algorithm for unsupervised domain generalization. Generally, we pretrain DIUL on the unlabeled dataset S_{UL} before finetuning with the labeled dataset S_{L} . The finetuning phase can be considered as a standard DG setting thus any DG method such as [29, 39, 46] can be applied. We focus on exploring how unsupervised learning helps models generalize to unseen domains.

Let $S_{\text{UL}} = \{X_n, d_n\}_{n=1}^N$ be the unlabeled dataset with a set of N images with domain labels but without the ground-truth category labels. Tsai et al. [57] has shown that the traditional contrastive learning could be modeled by:

$$P(\mathbf{Y}|\mathbf{X}) = \prod_{n=1}^N p(y_n|X_n) = \prod_{n=1}^N \frac{\exp(\mathbf{v}_{y_n}^\top \mathbf{f}_n/\tau)}{\sum_{i=1}^N \exp(\mathbf{v}_i^\top \mathbf{f}_n/\tau)}. \quad (4)$$

Here each of the datapoint X_n is assigned with a unique surrogate label $y_n \in \{1, 2, \dots, N\}$, \mathbf{v}_{y_n} and \mathbf{f}_n are given by passing the input image \mathbf{X}_n to two encoder networks f_θ and $f_{\theta'}$. τ is the temperature hyperparameter that controls the concentration level. The graphical model is shown in Fig. 1(a).

The conditional probability given by Eqn. 4 leads to the standard contrastive learning loss. In particular, MoCo learns Eqn. 4 via InfoNCE loss by sampling negative samples as follows:

$$\mathcal{L}(\theta, \theta') = -\frac{1}{N} \sum_{i=1}^N \log \frac{\exp(\mathbf{v}_i^\top \mathbf{f}_i/\tau)}{\exp(\mathbf{v}_i^\top \mathbf{f}_i/\tau) + \sum_{k=1}^K \exp(\mathbf{q}_k^\top \mathbf{f}_i/\tau)} \quad (5)$$

where $\mathbf{q} \in \mathbb{R}^{K \times d}$ is a queue of negative samples with size K storing previous embeddings from $f_{\theta'}$.

However, traditional contrastive learning fails to model domain information. Specifically, the classifier $P(Y|\mathbf{X})$ may be different under different domain label D , which leads to model misspecification. Hence given domain label information, we consider the new graphical probability model described in Fig. 1(b).

Next, we give the concrete form of the two conditional probabilities as follows, the generation process of Y is given by:

$$P(y_n|X_n, D = d) = \frac{\exp(\mathbf{v}_{y_n,d}^\top \mathbf{f}_n/\tau)}{\sum_{i \in N_d} \exp(\mathbf{v}_{i,d}^\top \mathbf{f}_n/\tau)} = \frac{\exp(\mathbf{v}_{y_n}^\top \mathbf{f}_n/\tau)}{\sum_{i \in N_d} \exp(\mathbf{v}_i^\top \mathbf{f}_n/\tau)}, \quad (6)$$

where N_d is a collection of training sample id which belongs to domain d . And the second equation holds as we further assume the dictionary vectors $\mathbf{v}_{i,d}$ are domain irrelevant, i.e. $\mathbf{v}_{i,d} = \mathbf{v}_i$, which could be modeled by a single neural network across all domains.

And the generation process of D is given by:

$$P(D = d|X_n) = \text{softmax}(h(X_n; \Phi))_d, \quad (7)$$

where h could be represented as a learnable convolutional neural network parameterized by Φ .

Hence the likelihood could be obtained from combining Eqn. 6 and Eqn. 7 as follows:

$$P(y_n|X_n) = \mathbb{E}_{D \sim P(D|X_n)} P(y_n|X_n, D) \quad (8)$$

$$= \sum_d P(D = d|X_n) P(y_n|X_n, D = d) \quad (9)$$

$$= \sum_d w_{n,d} \frac{\exp(\mathbf{v}_{y_n}^\top \mathbf{f}_n/\tau)}{\sum_{i \in N_d} \exp(\mathbf{v}_i^\top \mathbf{f}_n/\tau)}. \quad (10)$$

where $w_{n,d} = P(D = d|X_n)$ is given by Eqn. 7. Noticing that $w_{n,d}$ implies the similarity between domains via each sample, hence Eqn. 10 eliminates the relevance of domains by reweighting loss on different domains.

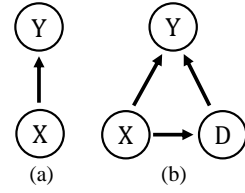


Figure 1: The graphical model of traditional contrastive learning (a) and our method (b).

Similar to Eqn. 5, we write our loss function as:

$$\mathcal{L}(\theta, \theta') = -\frac{1}{N} \sum_{i=1}^N \log \sum_d w_{i,d} \frac{\exp(\mathbf{v}_i^\top \mathbf{f}_i / \tau)}{\exp(\mathbf{v}_i^\top \mathbf{f}_i / \tau) + \sum_{k \in N_d, k \neq i} \exp(\mathbf{q}_k^\top \mathbf{f}_i / \tau)}. \quad (11)$$

In the processing of optimization, we first learn Φ by Eqn.7. With a given Φ we optimize θ via minimizing Eqn. 12 until convergence.

4 Experiments

In this section, we specifically describe experimental settings that support unsupervised domain generalization (UDG). We conduct extensive experiments on 3 UDG settings which are more common in real-world scenarios, namely *all correlated*, *domain correlated* and *uncorrelated*. Experiments on the *category correlated* setting are in Appendix B.1.

4.1 Unsupervised Domain Generalization (UDG)

Datasets and settings. We adopt 4 datasets to carry through these two settings, namely DomainNet [44], PACS [32], CIFAR-10-C and CIFAR-100-C [25, 31]. Introduction to these datasets and details of implementation are in Appendix A.1. We consider 3 settings of UDG, where the correlations between unlabeled and labeled data gradually decreases, namely *all correlated*, *domain correlated* and *uncorrelated*.

All correlated UDG.

We explore how unsupervised learning helps the generalization ability of models when training data are partially labeled and both the category and domain between unlabeled and labeled data are correlated.

We adopt DomainNet and PACS for this setting. For DomainNet, we randomly select 3 out of 6 domains as source domains and the remaining as target domains. 20 out of 300 categories are randomly selected for both training and testing. For PACS, we follow the common DG setting where one domain is considered as the target domain while the others as source domains for each run. Proportion of labeled data to training data for both datasets varies from 1% to 10%.

Results are shown in Table 1 (DomainNet) and 2 (PACS). DIUL outperforms other counterparts with all given fractions of labeled data on DomainNet and 3 out of 4 fractions on PACS. Surprisingly, when all the training data are labeled, unsupervised pretraining with the same data improves the prediction accuracy on target domains by a noticeable margin. This indicates that when there are severe distribution shifts between training and testing data, the supervision from category labels of source domains is insufficient given that it can be considered as biased knowledge in target domains. Unsupervised learned dissimilarities among samples from the same category in source domains can introduce valid knowledge for distinguishing categories in target domains, for which unsupervised learning naturally fit the DG problem.

Moreover, from the perspective of the graphical model mentioned in Section 3.2, supervision from source domain helps model to learn a domain relevant classifier, which can fail in target domains. While DIUL learns a domain irrelevant representation space leading to more robust predictions in novel domains. Thus DIUL achieves a significant improvement compared to SOTA unsupervised learning methods (7.43% compared to MoCo V2 and 3.89% to SimCLR V2).

When the fraction of labeled data is lower than 10%, we only finetune the linear classifier for all the methods to prevent overfitting. Both random initialized ResNet-18 and BYOL fail to learn a valid model with label fraction of 1% and 5%, while DIUL consistently achieves considerable improvement. Here we report the results of one of the possible divisions. Details of the data partition and results of other divisions are in Appendix A.2.

Domain correlated UDG.

Domain correlated UDG is a challenging setting with a great degree of flexibility, where unlabeled data can be sampled from other categories or even other datasets compared with labeled data as long as they share the same domain space. This setting is quite common in real-world scenarios given when category space is unknown one can hardly assume that the unlabeled data share the same

Table 1: Results of the *all correlated* setting on DomainNet. We reimplement state-of-the-art unsupervised methods on DomainNet with ResNet18 [21] as the backbone network for all the methods unless otherwise specified. ERM indicates the randomly initialized ResNet18. Overall and Avg. indicate the overall accuracy of all the test data and the arithmetic mean of the accuracy of 3 domains, respectively. Note that they are different because the capacities of different domains are not equal. The reported results are average over three repetitions of each run. All the models are trained on ‘Painting’, ‘Real’, and ‘Sketch’ domains of DomainNet and tested on the other three domains. The title of each column indicates the name of the domain used as target. All the models are pretrained for 1000 epoches before finetuned on the labeled data. The best results of all methods are highlighted with the bold font.

method	Label Fraction 1%					Label Fraction 5%				
	Clipart	Infograph	Quickdraw	Overall	Avg.	Clipart	Infograph	Quickdraw	Overall	Avg.
MoCo V2 [7, 22]	18.85	10.57	6.32	10.05	11.92	28.13	13.79	9.67	14.56	17.20
SimCLR V2 [6]	23.51	15.42	5.29	11.80	14.74	34.03	17.17	10.88	17.32	20.69
BYOL [18]	6.21	3.48	4.27	4.45	4.65	9.60	5.09	6.02	6.49	6.90
AdCo [27]	16.16	12.26	5.65	9.57	11.36	30.77	18.65	7.75	15.44	19.06
ERM	6.54	2.96	5.00	4.75	4.83	10.21	7.08	5.34	6.81	7.54
DIUL (ours)	18.53	10.62	12.65	13.29	13.93	39.32	19.09	10.50	18.73	22.97
Label Fraction 10%										
method	Clipart	Infograph	Quickdraw	Overall	Avg.	Clipart	Infograph	Quickdraw	Overall	Avg.
	32.46	18.54	8.05	15.92	19.69	64.18	27.44	25.26	33.76	38.96
MoCo V2	37.11	19.87	12.33	19.45	23.10	68.72	27.60	30.56	37.47	42.29
SimCLR V2	14.55	8.71	5.95	8.46	9.74	54.44	23.70	20.42	28.23	32.86
BYOL	32.25	17.96	11.56	17.53	20.59	62.84	26.69	26.26	33.80	38.60
AdCo	15.10	9.39	7.11	9.36	10.53	52.79	23.72	19.05	27.19	31.85
ERM	35.15	20.88	15.69	21.08	23.91	72.79	32.01	33.75	41.19	46.18

Table 2: Results of the *all correlated* setting on PACS. Given the experiment for each target domain is run respectively, there is no overall accuracy across domains. Thus we report the average accuracy and the accuracy for each domain. For details about the number of runs, meaning of column titles and fonts, see Table 1.

method	Label Fraction 1%					Label Fraction 5%				
	Photo	Art.	Cartoon	Sketch	Avg.	Photo	Art.	Cartoon	Sketch	Avg.
MoCo V2	22.97	15.58	23.65	25.27	21.87	37.39	25.57	28.11	31.16	30.56
SimCLR V2	30.94	17.43	30.16	25.20	25.93	54.67	35.92	35.31	36.84	40.68
BYOL	11.20	14.53	16.21	10.01	12.99	26.55	17.79	21.87	19.65	21.47
AdCo	26.13	17.11	22.96	23.37	22.39	37.65	28.21	28.52	30.35	31.18
ResNet-18	10.90	11.21	14.33	18.83	13.82	14.15	18.67	13.37	18.34	16.13
DIUL (ours)	27.78	19.82	27.51	29.54	26.16	44.61	39.25	36.41	36.53	39.20
Label Fraction 10%										
method	Photo	Art.	Cartoon	Sketch	Avg.	Photo	Art.	Cartoon	Sketch	Avg.
	44.19	25.85	33.53	24.97	32.14	59.86	28.58	48.89	34.79	43.03
MoCo V2	54.65	37.65	46.00	28.25	41.64	67.45	43.60	54.48	34.73	50.06
SimCLR V2	27.01	25.94	20.98	19.69	23.40	41.42	23.73	30.02	18.78	28.49
BYOL	46.51	30.21	31.45	22.96	32.78	58.59	29.81	50.19	30.45	42.26
AdCo	16.27	16.62	18.40	12.01	15.82	43.29	24.27	32.62	20.84	30.26
ResNet-18	53.37	39.91	46.41	30.17	42.47	68.66	41.53	56.89	37.51	51.15

categories with labeled data. We use this setting to validate the generalization ability of unsupervised learning methods under both domain and category shifts.

We adopt DomainNet for this setting given that the category spaces of other popular DG datasets (such as PACS, VLCS [56] and Office-home [58]) are limited. We randomly select 3 out of 6 domains as source domains and remaining domains are considered as target. We choose 20 out of 300 categories for labeled training and testing data, and other 40 or 100 categories for unlabeled data. There is no overlap between categories in unlabeled and labeled data, leading to the most challenging scenario in this setting. Details of data proportion and more experimental results are in Appendix A.3.

Results are shown in Table 3. DIUL achieves highest generalization accuracy on all of the domains. As aforementioned, current contrastive loss not only enlarge the distance between representations of samples from different categories but also that of samples from different domains. But the representations of domains being more distinguishable brings no benefit on downstream tasks [41]. On the contrary, DIUL forces the model to learn a domain irrelevant representation space where only representations from different latent categories can be easily distinguished. Intuitively, DIUL learns two kinds of abilities: 1) selecting domain irrelevant features which are most likely related to categories, and generating a latent representation space with them; 2) discerning domain related features and preventing them from contributing to the representation space. As a result, DIUL shows strong generalization ability under both domain and category shifts.

Table 3: Results of the *domain correlated* setting on DomainNet. For details about the number of runs, meaning of column titles and fonts, see Table 1.

method	Pretraining with data from 40 categories					Pretraining with data from 100 categories				
	Clipart	Infograph	Quickdraw	Overall	Avg.	Clipart	Infograph	Quickdraw	Overall	Avg.
MoCo V2	72.84	33.40	34.20	41.19	46.82	77.03	37.68	35.25	43.71	49.98
SimCLR V2	75.58	35.52	37.08	43.83	49.39	79.70	38.88	38.89	46.50	52.49
BYOL	58.39	23.99	28.56	32.87	36.98	58.27	24.14	27.83	32.49	36.75
AdCo	76.61	31.55	33.42	40.96	47.19	75.19	33.76	38.51	43.77	49.15
ERM	55.78	22.40	25.75	30.43	34.64	55.78	22.40	25.75	30.43	34.64
DIUL (ours)	78.40	33.98	39.87	44.20	50.75	82.28	40.60	47.68	52.19	56.85

Uncorrelated UDG

In this setting, we make no restrictions or assumptions about the correlation between unlabeled and labeled data. Thus unlabeled data can be sampled from novel domains, unknown categories or other datasets compared with labeled data. This brings great challenge to the generalization ability of models and the effectiveness of unsupervised learning given the mutual information between unlabeled and labeled data can reach minimum. Intuitively, with stronger connection between unlabeled and labeled data, unsupervised learning on unlabeled data brings greater improvement. We explore how unsupervised learning affect the generalization ability of models to novel domains when the distribution shifts between unlabeled and labeled data are significant.

Since the domain spaces of DomainNet and PACS are limited, we adopt CIFAR-100-C and CIFAR-10-C for this setting. In the most challenging scenario, the distribution of unlabeled data and labeled data can be uncorrelated, where we consider unlabeled CIFAR-100-C as the pretraining data and CIFAR-10-C for finetuning data and target data. To make the domain space sufficient, we generate distinguishing domains for CIFAR-100 and CIFAR-10 and there is no overlap among unlabeled training data, labeled training data and test data. As shown in Table 4, we randomly select 4 specific domains for pretraining, finetuning and test data, respectively, and set the severity level to 3. We adopt ResNet18 for this setting and the first layer was replaced by a convolution layer with kernel size of 3 and stride of 1, since size of images from CIFAR is 32×32 . Details of implementation and further experimental results when domains are differently selected are in Appendix A.4.

Results are shown in Table 4. Surprisingly, unsupervised pretraining methods achieve significant improvement though the pretraining data provides limited knowledge about labeled training and testing data. DIUL outperforms all the unsupervised learning counterparts on all the domains by a noticeable margin. The superiority of DIUL shows that samples even from different domains and categories compared to test data can help the model distinguish domain correlated features and category correlated features in the finetuning phase. In other words, similarities among category correlated features may help selecting predictive features while similarities among domain correlated features help model ignore category irrelevant features.

This largely broadens the valid scope of unsupervised learning given that no constrains of the category and source (domain) of pretraining data and labeled data are required to improve the model performance on novel domains.

Finetuning with DG methods Table 5 shows how unsupervised pretraining methods benefit the generalization ability of empirical risk minimization (ERM) models since all the finetuning phase of these method can be considered as the training phase of ERM models. Here we further explore how unsupervised training affects the models trained with effective domain generalization methods.

Table 4: Results of the *uncorrelated* setting on CIFAR. Pre. and Fine. are short for pretraining and finetuning data. E, F, I, and M donates ‘elastic’, ‘fog’, ‘impulse noise’ and ‘motion blur’, respectively. C, F, G, and S donates ‘contrast’, ‘frost’, ‘glass’, ‘blur’ and ‘shot noise’, respectively. For details about the number of runs, meaning of column titles and fonts, see Table 1.

method	Pre.	Fine.	Brightness	Defocus Blur	Gaussian Noise	Snow	Avg.
MoCo V2	E, F, I, M	C, F, G, S	77.13	75.88	75.18	72.27	75.12
SimCLR V2	E, F, I, M	C, F, G, S	78.54	77.60	75.92	72.68	76.19
BYOL	E, F, I, M	C, F, G, S	58.10	57.07	56.31	53.96	56.36
AdCo	E, F, I, M	C, F, G, S	75.63	77.32	78.84	72.25	76.01
ERM	E, F, I, M	C, F, G, S	36.53	34.61	33.49	32.98	34.40
DIUL (ours)	E, F, I, M	C, F, G, S	80.28	77.74	79.65	77.76	78.86

We report the results of state-of-the-art methods of domain generalization with unsupervised trained parameters as the initial state in Table 5. More experimental results are in Appendix A.5.

Table 5: Results of state-of-the-art methods with different initialization methods under the *domain correlated* setting on DomainNet. For details about the number of runs, meaning of column titles and fonts, see Table 1.

method	Clipart	Infograph	Quickdraw	Overall	Avg.
M-ADA [46]	65.33	37.51	30.16	38.75	44.33
RSC [29]	61.25	23.27	27.48	31.52	37.33
MMLD [39]	74.09	36.09	33.44	42.46	47.88
MoCo V2 + RSC	81.36	37.59	41.38	46.81	53.44
MoCo V2 + MMLD	82.46	39.52	40.58	47.83	54.19
DIUL (ours) + RSC	86.47	39.00	45.71	49.71	57.06
DIUL (ours) + MMLD	85.53	38.14	44.08	48.62	55.92

4.2 Comparison with ImageNet Pretrained Models

Comparison of models pretrained with various amounts of data As the amount of available unlabeled data grows, unsupervised pretraining achieves better performance. Surprisingly, we find it is possible for DIUL to outperform models pretrained on ImageNet though our unlabeled training data is of significantly smaller amount compared to ImageNet. Actually if we consider ImageNet as a mixture of data sampled from latent domains, the heterogeneity is limited for learning a generalizable model with a domain-irrelevant representation space [23]. Given data with strong heterogeneity (such as a subset of DomainNet), although there are strong distribution shifts between training data and testing data, DIUL can still learn domain-irrelevant representations and strengthen the generalization ability to target domains. As shown in Figure 2a, when the available data for pretraining are more than 100 out of 300 categories from DomainNet, DIUL outperforms ImageNet pretrained initialization by a noticeable margin. Note that the number of data that DIUL uses for pretraining is less than 1/10 of the number of ImageNet data. This observation indicates that stronger unsupervised pretrained models can be alternatives to the ones pretrained on ImageNet as the initialization approach for DG tasks.

4.3 Analysis

Visualization of representations We compare the embedding spaces learned by MoCo V2, DIUL and ImageNet pretraining protocol in Figure 3. Both MoCo V2 and DIUL are pretrained under the *domain correlated* setting for 1000 epochs, and we adopt t-SNE [36] visualization to compare how representations from different domains are distributed in the embedding spaces. ImageNet pretraining learns a embedding space where domains are clearly distinguishable, which is understandable since if we consider domains as categories, ImageNet pretrained models should have the ability to distinguish them given domains in DomainNet are highly distinguishable. MoCo V2 learns a more ‘dense’ embedding space where samples from domain ‘real’ and domain ‘painting’ are entangled closer compared to ImageNet pretraining protocol, but samples from domain ‘sketch’ are separated from others. On the contrary, in the embedding space learned via DIUL, samples from different domains

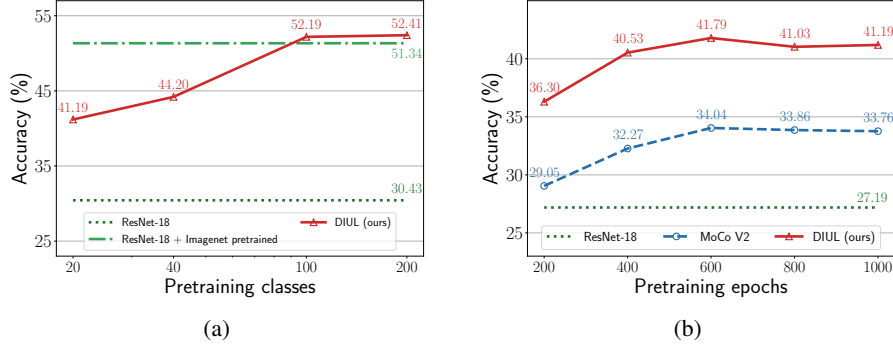


Figure 2: Figure (a) shows how the generalization accuracy of DIUL grows as the amount of available data increases. All the models are pretrained with DIUL for 600 epochs. Pretraining classes indicates the number of categories used in the pretraining phase. DIUL outperforms models with ImageNet pretrained weights as the initialization when the number of available categories reaches 100. Figure (b) shows the convergence speed of MoCo V2 and DIUL. Pretraining epoch is the number of epoch for pretraining. DIUL is more time efficient and achieves considerable higher generalization accuracy after convergence.

are closely entangled together, clearly indicating that DIUL learns a domain irrelevant representation space.

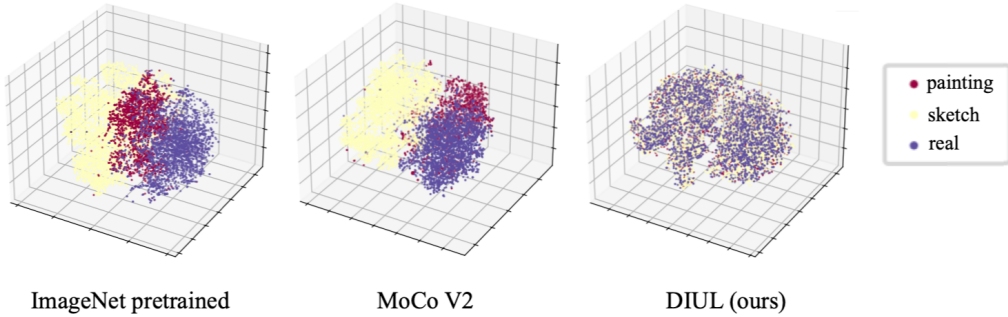


Figure 3: T-SNE of different initialization methods. Ours method learns a domain-irrelevant representation space.

Comparison of DIUL and MoCo V2 Figure 2b visualizes the accuracy on the *all correlated* setting under various pretraining epochs. All the parameters and pretraining protocol used for both methods are the same for a fair comparison. With a small number of pretraining epochs, DIUL outperforms MoCo V2 by a considerable margin. As the number of pretraining epochs grows, MoCo V2 reaches a maximal overall accuracy of 34.04% after pretraining for 600 epochs before the curve tends to be flat, while DIUL outperforms MoCo V2 by around 7.43% at epoch 1000. The curve indicates that DIUL is not only a efficient pretraining method but also with a better convergence point.

5 Conclusion

In this paper, we proposed a novel problem called unsupervised domain generalization (UDG), where unlabeled data are used to strengthen the generalization ability of models since labeled data are usually costly or unavailable. We also proposed a domain-irrelevant representation learning method called DIUL to address the UDG problem. Extensive experiments clearly demonstrated the effectiveness of the proposed DIUL compared with state-of-the-art unsupervised learning counterparts. As a pretraining approach, DIUL outperforms ImageNet pretraining approach with significantly less data, showing a encouraging way to initialize models for the DG problem.

References

- [1] Martin Arjovsky, Léon Bottou, Ishaaan Gulrajani, and David Lopez-Paz. Invariant risk minimization. *arXiv preprint arXiv:1907.02893*, 2019.
- [2] Philip Bachman, R Devon Hjelm, and William Buchwalter. Learning representations by maximizing mutual information across views. *arXiv preprint arXiv:1906.00910*, 2019.
- [3] Yoshua Bengio, Tristan Deleu, Nasim Rahaman, Nan Rosemary Ke, Sébastien Lachapelle, Olexa Bilaniuk, Anirudh Goyal, and Christopher Pal. A meta-transfer objective for learning to disentangle causal mechanisms. In *International Conference on Learning Representations*, 2019.
- [4] Fabio M Carlucci, Antonio D’Innocente, Silvia Bucci, Barbara Caputo, and Tatiana Tommasi. Domain generalization by solving jigsaw puzzles. In *Proceedings of the IEEE/CVF Conference on Computer Vision and Pattern Recognition*, pages 2229–2238, 2019.
- [5] Ting Chen, Simon Kornblith, Mohammad Norouzi, and Geoffrey Hinton. A simple framework for contrastive learning of visual representations. In *International conference on machine learning*, pages 1597–1607. PMLR, 2020.
- [6] Ting Chen, Simon Kornblith, Kevin Swersky, Mohammad Norouzi, and Geoffrey Hinton. Big self-supervised models are strong semi-supervised learners. *arXiv preprint arXiv:2006.10029*, 2020.
- [7] Xinlei Chen, Haoqi Fan, Ross Girshick, and Kaiming He. Improved baselines with momentum contrastive learning. *arXiv preprint arXiv:2003.04297*, 2020.
- [8] Carl Doersch, Abhinav Gupta, and Alexei A Efros. Unsupervised visual representation learning by context prediction. In *Proceedings of the IEEE international conference on computer vision*, pages 1422–1430, 2015.
- [9] Jeff Donahue, Philipp Krähenbühl, and Trevor Darrell. Adversarial feature learning. *arXiv preprint arXiv:1605.09782*, 2016.
- [10] Alexey Dosovitskiy, Jost Tobias Springenberg, Martin Riedmiller, and Thomas Brox. Discriminative unsupervised feature learning with convolutional neural networks. Citeseer, 2014.
- [11] Qi Dou, Daniel Coelho de Castro, Konstantinos Kamnitsas, and Ben Glocker. Domain generalization via model-agnostic learning of semantic features. In *Advances in Neural Information Processing Systems*, volume 32. Curran Associates, Inc., 2019.
- [12] Qi Dou, Daniel Coelho de Castro, Konstantinos Kamnitsas, and Ben Glocker. Domain generalization via model-agnostic learning of semantic features. In *Advances in Neural Information Processing Systems*, volume 32. Curran Associates, Inc., 2019.
- [13] Vincent Dumoulin, Ishmael Belghazi, Ben Poole, Olivier Mastropietro, Alex Lamb, Martin Arjovsky, and Aaron Courville. Adversarially learned inference. *arXiv preprint arXiv:1606.00704*, 2016.
- [14] Logan Engstrom, Brandon Tran, Dimitris Tsipras, Ludwig Schmidt, and Aleksander Madry. Exploring the landscape of spatial robustness. In *International Conference on Machine Learning*, pages 1802–1811. PMLR, 2019.
- [15] Zhe Gan, Yen-Chun Chen, Linjie Li, Chen Zhu, Yu Cheng, and Jingjing Liu. Large-scale adversarial training for vision-and-language representation learning. In H. Larochelle, M. Ranzato, R. Hadsell, M. F. Balcan, and H. Lin, editors, *Advances in Neural Information Processing Systems*, volume 33, pages 6616–6628. Curran Associates, Inc., 2020.
- [16] Muhammad Ghifary, W Bastiaan Kleijn, Mengjie Zhang, and David Balduzzi. Domain generalization for object recognition with multi-task autoencoders. In *Proceedings of the IEEE international conference on computer vision*, pages 2551–2559, 2015.

- [17] Ian J Goodfellow, Jean Pouget-Abadie, Mehdi Mirza, Bing Xu, David Warde-Farley, Sherjil Ozair, Aaron Courville, and Yoshua Bengio. Generative adversarial networks. *arXiv preprint arXiv:1406.2661*, 2014.
- [18] Jean-Bastien Grill, Florian Strub, Florent Altché, Corentin Tallec, Pierre Richemond, Elena Buchatskaya, Carl Doersch, Bernardo Avila Pires, Zhaohan Guo, Mohammad Gheshlaghi Azar, Bilal Piot, koray kavukcuoglu, Remi Munos, and Michal Valko. Bootstrap your own latent - a new approach to self-supervised learning. In H. Larochelle, M. Ranzato, R. Hadsell, M. F. Balcan, and H. Lin, editors, *Advances in Neural Information Processing Systems*, volume 33, pages 21271–21284. Curran Associates, Inc., 2020.
- [19] Ishaan Gulrajani and David Lopez-Paz. In search of lost domain generalization. *arXiv preprint arXiv:2007.01434*, 2020.
- [20] Ben Harwood, Vijay Kumar BG, Gustavo Carneiro, Ian Reid, and Tom Drummond. Smart mining for deep metric learning. In *Proceedings of the IEEE International Conference on Computer Vision*, pages 2821–2829, 2017.
- [21] Kaiming He, Xiangyu Zhang, Shaoqing Ren, and Jian Sun. Deep residual learning for image recognition. In *Proceedings of the IEEE conference on computer vision and pattern recognition*, pages 770–778, 2016.
- [22] Kaiming He, Haoqi Fan, Yuxin Wu, Saining Xie, and Ross Girshick. Momentum contrast for unsupervised visual representation learning. In *Proceedings of the IEEE/CVF Conference on Computer Vision and Pattern Recognition*, pages 9729–9738, 2020.
- [23] Yue He, Zheyuan Shen, and Peng Cui. Towards non-iid image classification: A dataset and baselines. *Pattern Recognition*, 110:107383, 2021.
- [24] Olivier Henaff. Data-efficient image recognition with contrastive predictive coding. In *International Conference on Machine Learning*, pages 4182–4192. PMLR, 2020.
- [25] Dan Hendrycks and Thomas Dietterich. Benchmarking neural network robustness to common corruptions and perturbations. In *International Conference on Learning Representations*, 2018.
- [26] R Devon Hjelm, Alex Fedorov, Samuel Lavoie-Marchildon, Karan Grewal, Phil Bachman, Adam Trischler, and Yoshua Bengio. Learning deep representations by mutual information estimation and maximization. In *International Conference on Learning Representations*, 2018.
- [27] Qianjiang Hu, Xiao Wang, Wei Hu, and Guo-Jun Qi. Adco: Adversarial contrast for efficient learning of unsupervised representations from self-trained negative adversaries. *arXiv preprint arXiv:2011.08435*, 2020.
- [28] Shoubo Hu, Kun Zhang, Zhitang Chen, and Laiwan Chan. Domain generalization via multidomain discriminant analysis. In *Uncertainty in Artificial Intelligence*, pages 292–302. PMLR, 2020.
- [29] Zeyi Huang, Haohan Wang, Eric P Xing, and Dong Huang. Self-challenging improves cross-domain generalization. *arXiv preprint arXiv:2007.02454*, 2, 2020.
- [30] Aditya Khosla, Tinghui Zhou, Tomasz Malisiewicz, Alexei A Efros, and Antonio Torralba. Undoing the damage of dataset bias. In *European Conference on Computer Vision*, pages 158–171. Springer, 2012.
- [31] Alex Krizhevsky, Geoffrey Hinton, et al. Learning multiple layers of features from tiny images. 2009.
- [32] Da Li, Yongxin Yang, Yi-Zhe Song, and Timothy M Hospedales. Deeper, broader and artier domain generalization. In *Proceedings of the IEEE international conference on computer vision*, pages 5542–5550, 2017.
- [33] Da Li, Yongxin Yang, Yi-Zhe Song, and Timothy Hospedales. Learning to generalize: Meta-learning for domain generalization. In *Proceedings of the AAAI Conference on Artificial Intelligence*, volume 32, 2018.

- [34] Da Li, Jianshu Zhang, Yongxin Yang, Cong Liu, Yi-Zhe Song, and Timothy M Hospedales. Episodic training for domain generalization. In *Proceedings of the IEEE/CVF International Conference on Computer Vision*, pages 1446–1455, 2019.
- [35] Haoliang Li, Sinno Jialin Pan, Shiqi Wang, and Alex C Kot. Domain generalization with adversarial feature learning. In *Proceedings of the IEEE Conference on Computer Vision and Pattern Recognition*, pages 5400–5409, 2018.
- [36] Shusen Liu, Dan Maljovec, Bei Wang, Peer-Timo Bremer, and Valerio Pascucci. Visualizing high-dimensional data: Advances in the past decade. *IEEE transactions on visualization and computer graphics*, 23(3):1249–1268, 2016.
- [37] Massimiliano Mancini, Samuel Rota Bulò, Barbara Caputo, and Elisa Ricci. Best sources forward: domain generalization through source-specific nets. In *2018 25th IEEE international conference on image processing (ICIP)*, pages 1353–1357. IEEE, 2018.
- [38] Massimiliano Mancini, Samuel Rota Bulo, Barbara Caputo, and Elisa Ricci. Robust place categorization with deep domain generalization. *IEEE Robotics and Automation Letters*, 3(3):2093–2100, 2018.
- [39] Toshihiko Matsuura and Tatsuya Harada. Domain generalization using a mixture of multiple latent domains. In *Proceedings of the AAAI Conference on Artificial Intelligence*, volume 34, pages 11749–11756, 2020.
- [40] Saeid Motiian, Marco Piccirilli, Donald A Adjeroh, and Gianfranco Doretto. Unified deep supervised domain adaptation and generalization. In *Proceedings of the IEEE international conference on computer vision*, pages 5715–5725, 2017.
- [41] Krikamol Muandet, David Balduzzi, and Bernhard Schölkopf. Domain generalization via invariant feature representation. In *International Conference on Machine Learning*, pages 10–18. PMLR, 2013.
- [42] Mehdi Noroozi and Paolo Favaro. Unsupervised learning of visual representations by solving jigsaw puzzles. In *European conference on computer vision*, pages 69–84. Springer, 2016.
- [43] Aaron van den Oord, Yazhe Li, and Oriol Vinyals. Representation learning with contrastive predictive coding. *arXiv preprint arXiv:1807.03748*, 2018.
- [44] Xingchao Peng, Qinxun Bai, Xide Xia, Zijun Huang, Kate Saenko, and Bo Wang. Moment matching for multi-source domain adaptation. In *Proceedings of the IEEE/CVF International Conference on Computer Vision*, pages 1406–1415, 2019.
- [45] Vihari Piratla, Praneeth Netrapalli, and Sunita Sarawagi. Efficient domain generalization via common-specific low-rank decomposition. In *International Conference on Machine Learning*, pages 7728–7738. PMLR, 2020.
- [46] Fengchun Qiao, Long Zhao, and Xi Peng. Learning to learn single domain generalization. In *Proceedings of the IEEE/CVF Conference on Computer Vision and Pattern Recognition*, pages 12556–12565, 2020.
- [47] Benjamin Recht, Rebecca Roelofs, Ludwig Schmidt, and Vaishaal Shankar. Do imagenet classifiers generalize to imagenet? In *International Conference on Machine Learning*, pages 5389–5400. PMLR, 2019.
- [48] Nikunj Saunshi, Orestis Plevrakis, Sanjeev Arora, Mikhail Khodak, and Hrishikesh Khanderkar. A theoretical analysis of contrastive unsupervised representation learning. In *International Conference on Machine Learning*, pages 5628–5637. PMLR, 2019.
- [49] Seonguk Seo, Yumin Suh, Dongwan Kim, Jongwoo Han, and Bohyung Han. Learning to optimize domain specific normalization for domain generalization. *arXiv preprint arXiv:1907.04275*, 3(6):7, 2019.
- [50] Harshay Shah, Kaustav Tamuly, Aditi Raghunathan, Prateek Jain, and Praneeth Netrapalli. The pitfalls of simplicity bias in neural networks. *arXiv preprint arXiv:2006.07710*, 2020.

- [51] Shiv Shankar, Vihari Piratla, Soumen Chakrabarti, Siddhartha Chaudhuri, Preethi Jyothi, and Sunita Sarawagi. Generalizing across domains via cross-gradient training. In *International Conference on Learning Representations*, 2018.
- [52] Kihyuk Sohn, David Berthelot, Chun-Liang Li, Zizhao Zhang, Nicholas Carlini, Ekin D Cubuk, Alex Kurakin, Han Zhang, and Colin Raffel. Fixmatch: Simplifying semi-supervised learning with consistency and confidence. *arXiv preprint arXiv:2001.07685*, 2020.
- [53] Jiawei Su, Danilo Vasconcellos Vargas, and Kouichi Sakurai. One pixel attack for fooling deep neural networks. *IEEE Transactions on Evolutionary Computation*, 23(5):828–841, 2019.
- [54] Yonglong Tian, Dilip Krishnan, and Phillip Isola. Contrastive multiview coding. *arXiv preprint arXiv:1906.05849*, 2019.
- [55] Yonglong Tian, Chen Sun, Ben Poole, Dilip Krishnan, Cordelia Schmid, and Phillip Isola. What makes for good views for contrastive learning. *arXiv preprint arXiv:2005.10243*, 2020.
- [56] Antonio Torralba and Alexei A Efros. Unbiased look at dataset bias. In *CVPR 2011*, pages 1521–1528. IEEE, 2011.
- [57] Tsung Wei Tsai, Chongxuan Li, and Jun Zhu. Mi{ce}: Mixture of contrastive experts for unsupervised image clustering. In *International Conference on Learning Representations*, 2021. URL https://openreview.net/forum?id=gV3wdEOGy_V.
- [58] Hemanth Venkateswara, Jose Eusebio, Shayok Chakraborty, and Sethuraman Panchanathan. Deep hashing network for unsupervised domain adaptation. In *Proceedings of the IEEE conference on computer vision and pattern recognition*, pages 5018–5027, 2017.
- [59] Pascal Vincent, Hugo Larochelle, Yoshua Bengio, and Pierre-Antoine Manzagol. Extracting and composing robust features with denoising autoencoders. In *Proceedings of the 25th international conference on Machine learning*, pages 1096–1103, 2008.
- [60] Shujun Wang, Lequan Yu, Caizi Li, Chi-Wing Fu, and Pheng-Ann Heng. Learning from extrinsic and intrinsic supervisions for domain generalization. In *European Conference on Computer Vision*, pages 159–176. Springer, 2020.
- [61] Chao-Yuan Wu, R Manmatha, Alexander J Smola, and Philipp Krahenbuhl. Sampling matters in deep embedding learning. In *Proceedings of the IEEE International Conference on Computer Vision*, pages 2840–2848, 2017.
- [62] Zhirong Wu, Yuanjun Xiong, Stella X Yu, and Dahua Lin. Unsupervised feature learning via non-parametric instance discrimination. In *Proceedings of the IEEE Conference on Computer Vision and Pattern Recognition*, pages 3733–3742, 2018.
- [63] Xingxuan Zhang, Peng Cui, Renzhe Xu, Linjun Zhou, Yue He, and Zheyang Shen. Deep stable learning for out-of-distribution generalization. *arXiv preprint arXiv:2104.07876*, 2021.
- [64] Kaiyang Zhou, Yongxin Yang, Timothy Hospedales, and Tao Xiang. Deep domain-adversarial image generation for domain generalisation. In *Proceedings of the AAAI Conference on Artificial Intelligence*, volume 34, pages 13025–13032, 2020.
- [65] Kaiyang Zhou, Yongxin Yang, Timothy Hospedales, and Tao Xiang. Learning to generate novel domains for domain generalization. In *European Conference on Computer Vision*, pages 561–578. Springer, 2020.

Method

As mentioned in Section 3.2, DUIL learns by minimizing loss:

$$\mathcal{L}(\theta, \theta') = -\frac{1}{N} \sum_{i=1}^N \log \sum_d w_{i,d} \frac{\exp(\mathbf{v}_i^\top \mathbf{f}_i / \tau)}{\exp(\mathbf{v}_i^\top \mathbf{f}_i / \tau) + \sum_{k \in N_d, k \neq i} \exp(\mathbf{q}_k^\top \mathbf{f}_i / \tau)}. \quad (12)$$

In recent contrastive learning methods, θ' can be identical[6], distinct[54] or the exponential moving average[22] of θ . Here we follow MoCo[22], where θ' is a momentum-based moving average of θ .

In practice, most contrastive learning methods maintains a collection of negative samples to generate negative pairs with positive queries. Current approaches of generating negative queries can be devided into three categories: 1) iteratively updating with the representations from the current minibatch in a First-In-First-Out (FIFO) manner[22]; 2) collecting all the negative samples from current minibatch[6]; 3) learning nagative queries adversarially[27].

As shown in Eqn. 12, we maintain domain specific negative queries to calculate similarity across domains. If the queue of negative representations are iteratively updated in a First-In-First-Out (FIFO) manner over minibatches, the number of samples from different domains can varies wildly, causing inconsistent queues of negative representations. If all of the negative samples come from current minibatch, queries for some domains can be minor since we make no assumption about the capacities of different domains. Thus we adopt a adversarial updating method to closely track the change of representations. Unlike [27] which maintains a global negative dictionary, we build several domain-specific negative sample sets only updated with the samples from corresponding domains. Thus our objective can be considered as:

$$\theta^*, \mathcal{Q}_1^*, \dots, \mathcal{Q}_D^* = \arg \min_{\theta} \max_{\mathcal{Q}_1, \dots, \mathcal{Q}_D} \mathcal{L}(\theta, \mathcal{Q}_1, \dots, \mathcal{Q}_D) \quad (13)$$

Specifically, we iteratively update network weights θ and domain-specific negative adversaries as follows:

$$\theta \leftarrow \theta - \eta_\theta \frac{\partial \mathcal{L}(\theta, \mathcal{Q}_1, \dots, \mathcal{Q}_D)}{\partial \theta} \quad (14)$$

$$\mathbf{q}_k \leftarrow \mathbf{q}_k + \eta_N \frac{\partial \mathcal{L}(\theta, \mathcal{Q}_1, \dots, \mathcal{Q}_D)}{\partial \mathbf{q}_k}, \quad \text{for } k \in N_d \quad (15)$$

where $k = 1, \dots, N_d$ is the index of negative sample, \mathcal{Q}_i is the set of samples whose indices are in N_d , η_θ and η_N are the learning rates for network weights and negative adversaries, respectively. Our objective is to maintain hard samples for positive ones in each domain, so the negative samples in a given domain are pushed closer towards the queries from the same domain, thus $n_{k,d}$ is optimized to maximize the similarities between them and positive queries within the corresponding domains and the learned negative sets closely track the change of representations from give domains.

A Experiments

A.1 Datasets and details of implementation

We adopt 4 datasets to conduct experiments in our 4 settings. We briefly introduce them as follows.

CIFAR-10-C and **CIFAR-100-C** are robustness benchmarks consisting of 19 corruptions types with five levels of severities. We select level 3 for all the experiments. Example images are shown in Fig. 4.

DomainNet is comprised of 6 domains, namely *clipart*, *infograph*, *painting*, *quickdraw*, *real*, *sketch*. It contains 586, 575 examples of size (3, 224, 224) and 345 classes. Example images are shown in Fig. 5.

PACS is a widely used benchmark for domain generalization which consists of 7 object categories spanning 4 image styles, namely *photo*, *art-painting*, *cartoon* and *sketch*. We adopt the protocol in [32] to split the training and val set. Example images are shown in Fig. 6.

Details of implementation. For all the experiments, we use ResNet-18 as the backbone network unless otherwise specified. The learning rate for pretraining is 0.03 and then decays with a cosine decay schedule. The weight decay is set to $1e^{-4}$ and the batch size is set to 1024. For *domain correlated* and *category correlated*, all methods are pretrained for 600 epochs, while for other settings 1000 epochs. We follow[7] for the augmentations and the optimization temperature. The feature dimension is set to 128. For finetuning, all methods are trained for 30 epochs for all the settings, while the learning rate and weight decay are set to $1e^{-3}$ and $1e^{-4}$, respectively.

A.2 All correlated UDG

Table 6: Results of the *all correlated* setting on DomainNet. We reimplement state-of-the-art unsupervised methods on DomainNet with ResNet18 [21] as the backbone network for all the methods. ERM indicates the randomly initialed ResNet18. Overall and Avg. indicate the overall accuracy of all the test data and the arithmetic mean of the accuracy of 3 domains, respectively. Note that they are different because the capacities of different domains are not equal. The reported results are average over three repetitions of each run. All of the models are trained on Clipart, Infograph, and Quickdraw domains of DomainNet and tested on the other three domains. The title of each column indicates the name of the domain used as target. All the models are pretrained for 1000 epoches before finetuned on the labeled data. The best results of all methods are highlighted with the bold font.

	Label Fraction 1%					Label Fraction 5%				
method	Painting	Real	Sketch	Overall	Avg.	Painting	Real	Sketch	Overall	Avg.
MoCo V2 [7, 22]	11.38	14.97	15.28	14.04	13.88	20.80	24.91	21.44	23.06	22.39
SimCLR V2 [6]	16.97	20.25	17.84	18.85	18.36	21.35	24.34	27.46	24.15	24.38
BYOL [18]	5.00	8.47	4.42	6.68	5.96	9.78	10.73	3.97	9.09	8.16
AdCo [27]	11.13	16.53	17.19	15.16	14.95	19.97	24.31	24.19	23.08	22.82
FixMatch [52]	12.25	12.98	15.56	13.30	13.60	21.59	26.01	27.32	25.67	24.97
ERM	6.68	6.97	7.25	6.94	6.96	7.45	6.08	5.00	6.24	6.18
DIUL (ours)	14.45	21.68	21.30	19.59	19.14	21.09	30.51	28.49	27.48	28.19
	Label Fraction 10%					Label Fraction 100%				
method	Painting	Real	Sketch	Overall	Avg.	Painting	Real	Sketch	Overall	Avg.
MoCo V2	25.35	29.91	23.71	27.37	26.32	43.42	58.61	40.38	50.66	47.47
SimCLR V2	24.01	30.17	31.58	28.75	28.59	46.79	62.32	51.05	55.71	53.39
BYOL	9.50	10.38	4.45	8.92	8.11	34.02	46.48	24.82	38.59	35.11
AdCo	23.35	29.98	27.57	27.65	26.97	43.55	61.42	51.23	54.37	52.07
FixMatch	25.15	32.39	33.18	30.54	30.24	44.76	55.15	54.93	52.22	51.62
ERM	9.90	9.19	5.12	8.56	8.07	31.50	40.21	24.01	34.48	31.91
DIUL (ours)	25.90	33.29	30.77	30.72	29.99	49.64	63.77	54.31	57.91	55.91

In Table 6 we show the effectiveness of unsupervised learning methods for DG on setting *all correlated* with when source domains are Clipart, Inforgraph and Quickdraw and target domains are Painting, Real and Sketch, respectively. Unsupervised training improves the generalization ability of models on the *All correlated UDG* setting. As explained in Section 4.1, this indicates the supervision from category labels of source domains is insufficient given that it can be considered as biased knowledge in target domains so that unsupervised pretraining is a effective approach for DG.

DIUL consistently outperforms other unsupervised learning counterparts with all of the the split manners of pretraining/fintuning subsets, showing the superior of domain irrelevant features against domain relevant features when generalizing to novel domains.

One can consider the *all correlated* setting as a semi-supervised domain generalization setting. Thus we compare DIUL with a SOTA semi-supervised method FixMatch[52]. DIUL outperforms FixMatch on almost all of the subsets. Note that semi-supervised methods such as FixMatch can only be applied to deal with the *all correlated* setting but not other settings such as the *uncorrelated* or the *domain*

correlated setting. DIUL shows much wider applicability compared to semi-supervised methods when the labeled data are heterogeneous and insufficient.

Details of data split are shown in Table 11, 12, 17, and 18.

A.3 Domain correlated UDG

Table 7: Results of the *domain correlated* setting on DomainNet. For details about the number of runs, meaning of column titles and fonts, see Table 6.

	Pretraining with data from 40 categories				
method	Painting	Real	Sketch	Overall	Avg.
MoCo V2	45.83	60.75	43.98	53.18	50.19
SimCLR V2	47.94	62.40	54.47	56.76	54.93
BYOL	33.73	45.63	25.48	38.21	34.95
AdCo	43.77	64.58	47.76	55.36	52.04
ERM	31.92	41.58	24.10	35.32	32.53
DIUL (ours)	47.82	65.07	56.90	58.61	56.60

We show that unsupervised learning improves models performance when the domains are re-split randomly in Table 7. DIUL achieves the best performance compared to other unsupervised methods, that indicates the superior of domain irrelevant features against domain relevant features when generalizing to novel domains.

A.4 Uncorrelated UDG

Table 8: Results of the *uncorrelated* setting on CIFAR. Pre. and Fine. are short for pretraining and finetuning data. B, D, G, and S denote Brightness, Defocus blur, Gaussian noise and Snow, respectively. C, F, G, and S donates Contrast, Frost, Glass, Blur and Shot noise, respectively. For details about the number of runs, meaning of column titles and fonts, see Table 6.

method	Pre.	Fine.	Elastic	Fog	Impulse Noise	Motion Blur	Avg.
MoCo V2	C, F, G, S	B, D, G, S	76.33	70.45	74.73	72.57	73.52
SimCLR V2	C, F, G, S	B, D, G, S	77.91	72.38	76.00	73.46	74.94
BYOL	C, F, G, S	B, D, G, S	58.32	50.88	54.34	56.95	55.13
AdCo	C, F, G, S	B, D, G, S	79.67	71.05	74.35	72.17	74.31
ERM	C, F, G, S	B, D, G, S	28.80	26.46	28.46	28.62	28.09
DIUL (ours)	C, F, G, S	B, D, G, S	78.98	71.52	76.65	73.19	75.09

We show that unsupervised learning improves models performance when the domains are re-split randomly on the *uncorrelated UDG* setting in Table 8. DIUL achieves the best performance compared to other unsupervised methods, that indicates the superior of domain irrelevant features against domain relevant features when generalizing to novel domains.

A.5 Finetuning with DG methods

Here we further explore how unsupervised training affects the models trained with effective domain generalization methods. We show that DIUL can be easily assembled with current DG methods to further improve the generalization ability.

Finetuning with DG methods Table 9 shows how unsupervised pretraining methods benefit the generalization ability of empirical risk minimization (ERM) models since all the finetuning phase of these method can be considered as the training phase of ERM models. Here we further explore how unsupervised training affects the models trained with effective domain generalization methods. We report the results of state-of-the-art methods of domain generalization with unsupervised trained parameters as the initial state in Table 9.

With unsupervised learning, DG methods show stronger generalization ability. As a strong initialization, DIUL learns a domain irrelevant embedding space which maintains prior knowledge about distinguishing between domain relevant and domain irrelevant features. Thus DIUL can help DG methods including RSC and MMLD learn stronger generalization ability to unseen domains.

If we consider DG methods as the backend of DIUL, they achieve better performance compared to finetuning methods with ERM, as shown in Table 9. Thus strong fully-supervised methods as the backend can further improve the performance of DIUL.

Then we compare DIUL with DG methods that enlarge the available data space with augmentations of source domains. The generation based methods learns to generate samples while training, so that they can easily handle tasks with simple inputs, such as MNIST dataset. But when the structure of source data are complex, such as large scale real-world images, generation based methods usually require considerable computation cost and the effectiveness is harmed. DIUL significantly outperforms generation based method such as M-ADA on the *domain correlated* setting, showing the superior of DIUL for real-world DG tasks.

Table 9: Results of state-of-the-art methods with different initialization methods under the *domain correlated* setting on DomainNet. For details about the number of runs, meaning of column titles and fonts, see Table 6.

method	Painting	Real	Sketch	Overall	Avg.
M-ADA [46]	31.24	44.96	25.51	37.17	33.90
RSC [29]	35.19	48.28	24.59	39.81	36.02
MMLD [39]	42.72	57.80	37.31	49.42	45.95
MoCo V2 + RSC	48.64	64.74	45.14	56.26	52.84
MoCo V2 + MMLD	51.57	65.75	50.52	58.70	55.94
DIUL (ours) + RSC	56.62	72.08	60.32	65.39	63.01
DIUL (ours) + MMLD	54.11	69.08	59.08	62.88	60.76

B Category correlated UDG

We present the forth UDG setting, namely *category correlated UDG*, where unlabeled and labeled data share the same category space but not the domain space. This setting has practical significance, given we can consider any kind of data structure of the source other than category, such as the batch of medical data generation or the time real-world images are taken, as domain. Thus data from different domains can share the same category space.

We use CIFAR-10-C for this setting since the domain spaces of DomainNet(6) and PACS(4) are limited. To make sure the category spaces of unlabeled and labeled data are correlated, we randomly select 60%, 20% and 20% of CIFAR-10 for pretraining, finetuning and test. We randomly select 4 specific domains for pretraining, finetuning and test data, respectively. The details of data split are in Table 16.

Results are shown in Table 10. Given pretraining, finetuning and test data share the same category space, the prior knowledge about category holds in the finetuning and inference phase. Thus unsupervised learning including MoVo V2, SimCLR V2 and BYOL achieve significant improvement for the *category correlated* setting. The embedding space DIUL learns maintains more prior knowledge about the category compared to other unsupervised methods since the DIUL prevents it from learning domain related features. So DIUL further improves the performance by 2.13%.

Table 10: Results of the *category correlated* setting on CIFAR. Pre. and Fine. are short for pretraining and finetuning data. B, C, E, and G denote Brightness, Contrast, Elastic and Gaussian noise, respectively. F, G, M, and S denote Frost, Glass Blur Motion blur and Snow, respectively. For details about the number of runs, meaning of column titles and fonts, see Table 6.

method	Pre.	Fine.	Defocus Blur	Fog	Impulse Noise	Shot Noise	Avg.
MoCo V2	B, C, E, G	F, G, M, S	76.90	73.67	73.33	76.54	75.11
SimCLR V2	B, C, E, G	F, G, M, S	80.26	75.39	76.48	79.43	77.89
BYOL	B, C, E, G	F, G, M, S	55.27	49.87	52.36	53.13	52.66
AdCo	B, C, E, G	F, G, M, S	77.96	75.33	75.62	77.89	76.70
ERM	B, C, E, G	F, G, M, S	26.53	23.34	25.67	27.94	25.87
DIUL (ours)	B, C, E, G	F, G, M, S	83.49	78.76	78.61	79.23	80.02

Table 11: Data split details of *all correlated* setting when source domains are Painting, Real and Sketch. Pretrain, finetune, test indicate the number of available samples from corresponding domains in the pretraining, finetuning and testing phase, respectively.

phase	Painting	Real	Sketch	Clipart	Infograph	Quickdraw	All.
pretrain	5305	9896	3901	0	0	0	19102
finetune	5305	9896	3901	0	0	0	19102
validation	600	1111	444	0	0	0	2155
test	0	0	0	3904	5348	10000	19252

Table 12: Data split details of *all correlated* setting when source domains are Clipart, Infograph and Quickdraw. Pretrain, finetune, test indicates the number of available samples from corresponding domains in the pretraining, finetuning and testing phase, respectively.

phase	Painting	Real	Sketch	Clipart	Infograph	Quickdraw	All.
pretrain	0	0	0	3504	4804	9000	17308
finetune	0	0	0	3504	4804	9000	17308
validation	0	0	0	400	544	1000	1944
test	5905	11007	4345	0	0	0	21257

Table 13: Data split details of *domain correlated* setting when source domains are Painting, Real and Sketch, while the number of class is 40. Pretrain, finetune, test indicate the number of available samples from corresponding domains in the pretraining, finetuning and testing phase, respectively.

phase	Painting	Real	Sketch	Clipart	Infograph	Quickdraw	All.
pretrain	9644	22421	10200	0	0	0	42265
finetune	4572	9726	4198	0	0	0	18496
validation	516	1092	478	0	0	0	2086
test	0	0	0	3471	5128	10000	18599

Table 14: Data split details of *domain correlated* setting when source domains are Clipart, Infograph and Quickdraw, while the number of class is 40. Pretrain, finetune, test indicate the number of available samples from corresponding domains in the pretraining, finetuning and testing phase, respectively.

phase	Painting	Real	Sketch	Clipart	Infograph	Quickdraw	All.
pretrain	0	0	0	5304	5625	20000	30929
finetune	0	0	0	3504	4804	9000	17308
validation	0	0	0	400	544	1000	1944
test	5905	11007	4345	0	0	0	21257

Table 15: Data split details of *domain correlated* setting when source domains are Painting, Real and Sketch, while the number of class is 100. Pretrain, finetune, test indicate the number of available samples from corresponding domains in the pretraining, finetuning and testing phase, respectively.

phase	Painting	Real	Sketch	Clipart	Infograph	Quickdraw	All.
pretrain	21213	49701	20868	0	0	0	91782
finetune	4572	9726	4198	0	0	0	18496
validation	516	1092	478	0	0	0	2086
test	0	0	0	3471	5128	10000	18599

Table 16: Data split details of *category correlated* setting. Pretrain, finetune, test indicate the number of available samples from corresponding domains in the pretraining, finetuning and testing phase, respectively.

phase	Brightness	Contrast	Elastic	Gaussian Noise	Frost	Glass Blur
pretrain	9000	9000	9000	9000	0	0
finetune	0	0	0	0	3000	3000
test	0	0	0	0	0	
phase	Motion Blur	Snow	Defocus Blur	Fog	Impulse Noise	Shot Noise
pretrain	0	0	0	0	0	0
finetune	3000	3000	0	0	0	0
test	0	0	3000	3000	3000	3000

Table 17: Category space of pretraining, finetuning and test for *all correlated* setting when source domains are Painting, Real and Sketch.

Phase	Available categories.
pretrain, finetune, test	The_Eiffel_Tower, bee, bird, blueberry, broccoli, fish, flower, giraffe, grass, hamburger, hexagon, horse, sun, tiger, toaster, tornado, train, violin, watermelon, zigzag

Table 18: Category space of pretraining, finetuning and test for *all correlated* setting when source domains are Clipart, Infograph and Quickdraw.

Phase	Available categories.
pretrain, finetune, test	The_Eiffel_Tower, bee, bird, blueberry, broccoli, fish, flower, giraffe, grass, hamburger, hexagon, horse, sun, tiger, toaster, tornado, train, violin, watermelon, zigzag

Table 19: Category space of pretraining, finetuning and test for *domain correlated* setting when source domains are Painting, Real and Sketch and the number of available category is 40.

Phase	Available categories.
pretrain	arm, backpack, basket, bear, beard, belt, bird, book, bridge, cat, cookie, couch, donut, drill, face, fan, finger, golf_club, grass, helicopter, jacket, key, keyboard, lighthouse, mailbox, marker, mug, pencil, pizza, potato, shoe, shovel, sink, skyscraper, spoon, squirrel, sweater, telephone, tiger, train
finetune, test	The_Eiffel_Tower, barn, bee, blueberry, broccoli, bus, butterfly, fish, giraffe, hamburger, hockey_stick, sea turtle, spider, toaster, tornado, triangle, violin, watermelon, wine_glass, zigzag

Table 20: Category space of pretraining, finetuning and test for *domain correlated* setting when source domains are Painting, Real and Sketch and the number of available category is 100.

Phase	Available categories.
pretrain	The_Great_Wall_of_China, The_Mona_Lisa, apple, arm, asparagus, baseball_bat, bathtub, belt, bicycle, binoculars, boomerang, bracelet, brain, bread, bucket, cake, calendar, candle, cannon, carrot, cat, ceiling_fan, chair, circle, crayon, crocodile, cruise_ship, cup, dolphin, door, dragon, dresser, elbow, elephant, eye, fire_hydrant, flamingo, flashlight, flip_flops, garden_hose, hammer, harp, helmet, hot_air_balloon, hourglass, house, kangaroo, knife, leg, light_bulb, lighter, line, mailbox, marker, microwave, monkey, moon, ocean, paintbrush, piano, pickup_truck, pliers, pond, pool, potato, rabbit, rain, rake, rifle, river, rollerskates, sailboat, sandwich, saxophone, school_bus, see_saw, shoe, sink, snail, snorkel, snowflake, soccer_ball, sock, spoon, square, string_bean, swing_set, table, telephone, tennis_racquet, tent, toe, toothbrush, toothpaste, tree, trombone, umbrella, vase, waterslide, windmill
finetune, test	The_Eiffel_Tower, barn, bee, blueberry, broccoli, bus, butterfly, fish, giraffe, hamburger, hockey_stick, sea turtle, spider, toaster, tornado, triangle, violin, watermelon, wine_glass, zigzag

Table 21: Category space of pretraining, finetuning and test for *domain correlated* setting when source domains are Clipart, Infograph and Quickdraw.

Phase	Available categories.
pretrain	arm, backpack, basket, bear, beard, belt, bird, book, bridge, cat, cookie, couch, donut, drill, face, fan, finger, golf_club, grass, helicopter, jacket, key, keyboard, lighthouse, mailbox, marker, mug, pencil, pizza, potato, shoe, shovel, sink, skyscraper, spoon, squirrel, sweater, telephone, tiger, train
finetune, test	The_Eiffel_Tower, bee, bird, blueberry, broccoli, fish, flower, giraffe, grass, hamburger, hexagon, horse, sun, tiger, toaster, tornado, train, violin, watermelon, zigzag

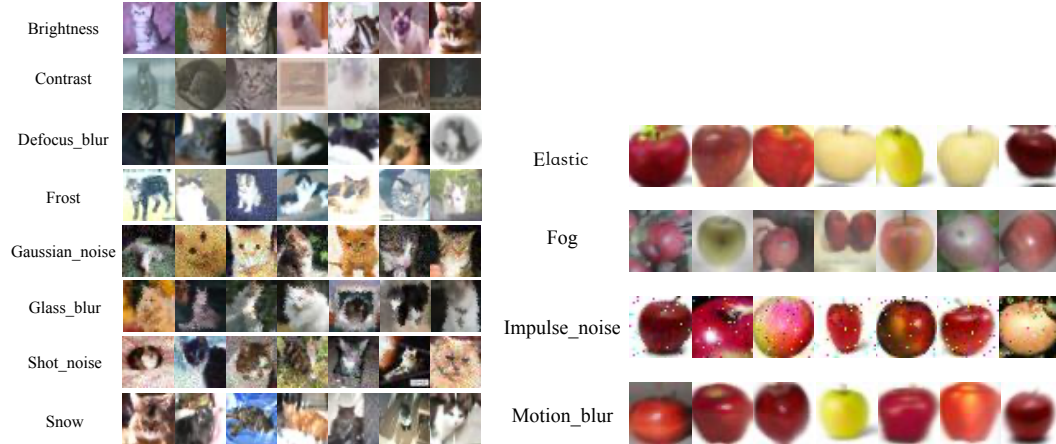


Figure 4: Example images of Cifar.

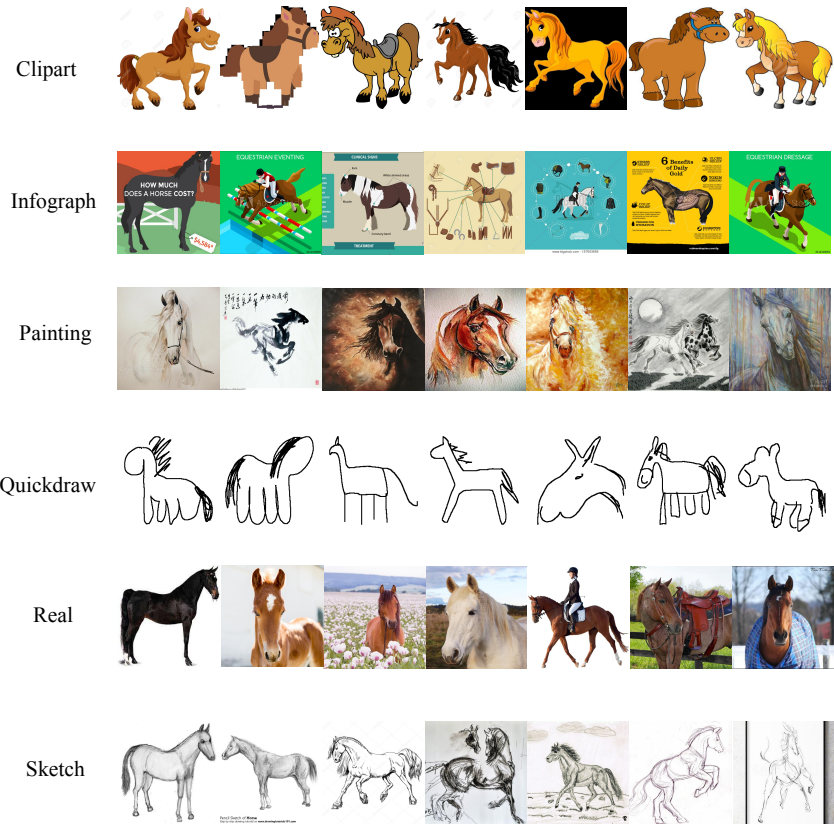


Figure 5: Example images of class horse in DomainNet.

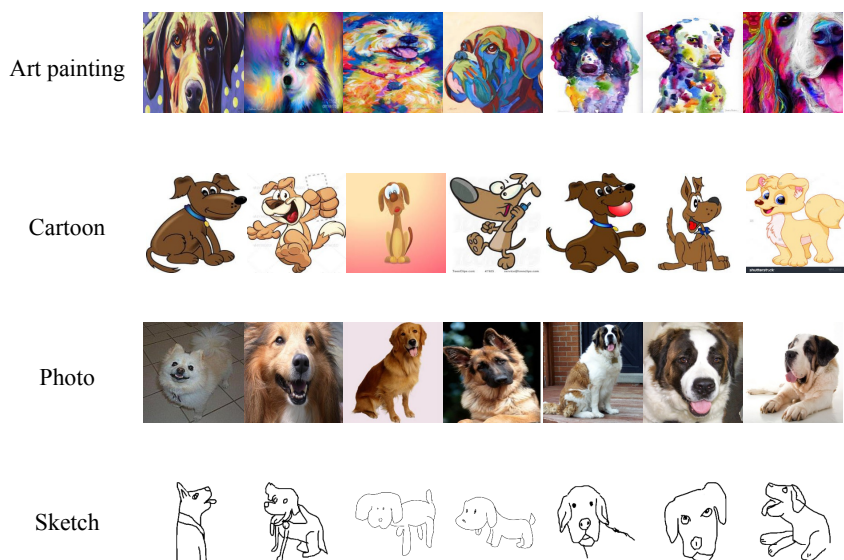


Figure 6: Example images of class dog in PACS.